Continuum Lowering and Fermi-Surface Rising in Strongly Coupled and Degenerate Plasmas

S. X. Hu (□□□)

Phys. Rev. Lett. **119**, 065001 — Published 10 August 2017

DOI: 10.1103/PhysRevLett.119.065001

Continuum Lowering and Fermi-Surface Rising in Strongly Coupled and Degenerate Plasmas

S. X. Hu (胡素兴)*

Laboratory for Laser Energetics, University of Rochester,

250 E. River Road, Rochester, NY 14623

*E-mail: shu@lle.rochester.edu

ABSTRACT

Continuum lowering is a well-known and important physics concept that describes the ionization potential depression (IPD) in plasmas caused by thermal-/pressure-induced ionization of outer-shell electrons. The existing IPD models are often used to characterize plasma conditions and to gauge opacity calculations. Recent precision measurements have revealed deficits in our understanding of continuum lowering in dense hot plasmas. However, these investigations have so far been limited to IPD in strongly coupled but nondegenerate plasmas. Here, we report a first-principles study of the K-edge shifting in both strongly coupled and fully degenerate carbon plasmas, with quantum molecular dynamics (QMD) calculations based on the all-electron density-functional theory (DFT). The resulted K-edge shifting *versus* plasma density, as a probe to the continuum lowering and the Fermi-surface rising, is found to be significantly different from predictions of existing IPD models. In contrast, a simple model of "*single-atom-in-box*" (SAIB), developed in this work, accurately predicts K-edge locations as what *ab-initio* calculations provide.

PACS: 52.27.Gr, 52.25.Os, 52.70.La, 52.25.-b

For an isolated neutral atom or atomic ion, the ionization potentials (IP's) of electrons represent the energies required to free these electrons from their bound states. If photons are used to ionize the 1*s*-core electron of atoms or atomic ions, the photoabsorption spectrum exhibits a sharp edge (the so-called "K edge") above which the ionization probability is increased by orders of magnitude. For an isolated atom or ion, the K edge generally characterizes the ionization potential of 1*s*-core electron. Namely, the K-edge location is determined by $E_{\text{K-edge}} = \text{IP} = E_C - E_{1s}$, with the continuum level E_C ($E_C = 0$ for an isolated atom or ion) and the binding energy E_{1s} of the 1*s*-core electron. If atoms are immersed into a plasma, the thermal-/pressure-induced ionization of outer-shell electrons can cause the "continuum" to lower. Once the atomic continuum is lowered in a plasma, the ionization potential of bound electrons seems to depreciate. The analytical models[1–4] of ionization potential depreciation (IPD) are often used to infer plasma density/temperature conditions by measuring atomic K-edges in plasmas. They have also been extensively applied to alter the detailed opacity and equation-of-state (EOS) calculations of plasmas.[5–8] Consequently, this well-known physics concept of continuum lowering[1–4] is very important not only to plasma physics but also to planetary science, astrophysics, and high-energy-density physics.

For its crucial importance to many fields, the IPD of atomic ions in plasmas has gained considerable attention over the past several years. These revisits have been motivated by recent experiments using both free-electron lasers to monitor K_α emission spectra at Linac Coherent Light Source (LCLS)[9–11] and the hot dense plasma experiment at ORION.[12] These precision experiments have revealed the lack of a consistent picture about continuum lowering in both solid-density aluminum plasmas and hot aluminum shocks at above-solid densities. In addition, a

recent x-ray Thomson-scattering experiment[13] has also indicated the enhanced ionization level in laser-driven shocks in polystyrene, even though it did not discriminate against different IPD models. The initial Linac Coherent Light Source (LCLS) experiments[9,10] favored the *ad hoc* Ecker–Kröll model[1] over the widely used Stewart–Pyatt model;[2] while the laser shock experiments at ORION[12] agreed better with the Stewart–Pyatt model[2] for pure Al plasmas. Moreover, a new experiment[14] at LCLS with other materials indicated that the Ecker–Kröll predictions of IPD for Mg plasma and Al compounds significantly disagree with experimental results. These measurements have stimulated a variety of theoretical studies.[15–18] Both experimental and theoretical studies have brought into question the accuracy of the standard density-dependent analytical models used to describe continuum lowering in hot solid-density and above-solid-density plasmas, highlighting an urgent need for an improved treatment of density effects in these plasmas.

These studies on continuum lowering have so far been limited, however, to coupled but nondegenerate plasmas. Other studies of the K-edge shape changes in warm dense plasmas[19–21] have been made, but only for solid density or moderate compression of solid targets by a single shock. How the K edge moves in both strongly coupled and degenerate (extremely dense) plasmas is another important question that remains to be answered. These plasma conditions are often found in astrophysical objects[22] and are now accessible at various high-energy-density (HED) physics facilities.[23] A thorough understanding of the physics of such strongly coupled and degenerate matter can have profound implications to many fields ranging from astrophysics,[22] planetary science,[24] and inertial confinement fusion[25–27] to HED physics.[28] In this report, we have applied the quantum molecular dynamics (QMD) method, based on the

finite-temperature density-functional theory (DFT),[29,30] to investigate the K-edge shifting of carbon plasmas under extreme compressions (ρ = 3 to 200 g/cm^3 and T = 1 to 50 eV). We found that the resulting K edges of strongly coupled and degenerate carbon plasmas significantly disagree with the existing continuum-lowering models as the carbon density increases. To understand the observed K-edge upshifting of extremely dense carbon plasmas, we have developed a simple model of "single-atom-in-box" (SAIB), which incorporates both the *ab initio* continuum lowering and the rising of the Fermi surface in these strongly coupled and degenerate plasmas. The SAIB model accurately predicts the K edges observed in our QMD calculations.

The K-edge shifting of extremely dense carbon plasmas: In our investigations, we take carbon as an example to explore how the K edge of atomic ions may change because of extremely high compressions. To calculate the optical properties of dense carbon plasmas, we employed the QMD method to simulate the plasma dynamics for thousands of steps. QMD, describing electrons quantum-mechanically with classical motions of ions, has been proven to be an accurate method for studying the properties of warm dense plasmas.[31–37] Different from most QMD studies of using projector-augmented-wave (PAW) pseudo-potential with "frozen" core-electrons, we applied the pure Coulombic potential for the electron–ion interactions in our all-electron DFT calculations, to have the 1*s*-core electrons participate in x-ray absorptions. To accurately sample the 1*s*-electron orbital, we increased the maximum plane-wave cutoff energy (ENMAX) ≥ 60 keV in our plane-wave–based QMD simulations. The static properties (pressure and internal-energy) from such Coulomb-potential QMD calculations agree well with PAW-pseudopotential calculations. The convergence was reached with this cutoff energy and by having at least 64 atoms in a supercell (see **Supplemental Material**[38]). Periodic boundary

condition is assumed in our QMD calculations. Once we obtained the plasma evolution after thousands of QMD steps, we took five to ten uncorrelated snapshots of the different ionic configurations to compute the optical property of dense carbon plasmas, using the Kubo–Greenwood formalism.[42] Averaging over these snapshots, we obtained the x-ray absorption spectra. Molecular-dynamics simulations are necessary to sample different ionic configurations of such warm-dense carbons in fluid-phase.

As an example, Fig. 1 shows the results from our QMD calculations, in which the mass absorption coefficient α_m is plotted as a function of the x-ray photon energy $h\nu$. Figures 1a–1d display the absorption spectra for carbon plasmas at different densities varying from ρ = 10 g/cm^3 to ρ =150 g/cm^3, respectively. The plasma temperature is set to T = 15,625 K for these calculations. For these density and temperature conditions, the ion–ion coupling parameter $\Gamma = Z^2e^2/4\pi\varepsilon_0 R_S kT$ is in the range of $\Gamma \approx 113.8$ to 680; while the degeneracy parameter $\theta = T/T_F$, varies from $\theta \approx 0.035$ to $\theta \approx 0.0035$. Here, $R_S = \left(3A_C/4\pi\rho\right)^{1/3}$ is the Wigner–Seitz radius with A_C being the mass of carbon atom and $kT_F = \left(\hbar^2/2m\right)\left(3\pi^2 \times Z \times \rho/A_C\right)^{2/3}$ is the Fermi energy with the ionization Z for each atom. As being indicated by Γ and θ, the dense carbon plasmas concerned are strongly coupled and fully degenerate. Figure 1 clearly shows that the x-ray absorption K edge of carbon shifts up as the density increases (see the black arrow in each panel). We see that the carbon K edge significantly shifts from $E_{\text{K-edge}}$ = 272.5 eV at ρ = 10 g/cm^3 to $E_{\text{K-edge}}$ = 442.5 eV at ρ = 150 g/cm^3.

For classical plasmas the K edge of an atomic ion can generally be calculated by $E_{\text{K edge}} = E_C - E_{1s}$, with only the lowered-continuum E_C and the binding energy of 1s electron of an

isolated atomic ion having a charge state of Z. In contrast to this, the K-edge in quantum degenerate plasmas also depends on the location of the Fermi surface. To look into why the K edge upshifts in the way displayed in Fig. 1, we have plotted the density of state (DOS) for the corresponding dense plasmas in Fig. 2. Setting the continuum level at energy zero (i.e., $E_C = 0$ for the Coulombic potential used), Fig. 2 shows the 1s band upshifted from $E_{1s} \approx -220$ eV at $\rho =$ 10 g/cm^3 to $E_{1s} = -$ (20 to 60) eV at $\rho = 150$ g/cm^3. This feature exactly accounts for the traditional picture of continuum lowering. Namely, the energy gap between the 1s-electron binding energy and the continuum is decreasing since pressure ionization occurs as density increases. As a consequence, the continuum lowering alone will give downshifted K edges with respect to the case of an isolated atomic ion at each individual charge state. In a drastic contrast to this traditional picture, the K edges are upshifted as ρ increases (see Fig. 1). The reason for the observed K-edge upshifting is attributed to the "rising" of the Fermi surface caused by high compressions. In Fig. 2, the vertical dashed lines mark the location of Fermi energy for each case. Now, the energy gap between the Fermi surface (E_F) and the 1s-orbital energy (E_{1s}) gives the exact K-edge locations seen in Fig. 1, e.g., $E_{\text{K-edge}} = E_F + E_C - E_{1s}$ (again here $E_C = 0$). Namely, for such degenerate quantum plasmas, the energy levels below E_F are fully occupied so that 1s electrons can be excited only by photons having an energy of $h\nu \geq (E_F - E_{1s})$. Therefore, the high compression leads to the rising of the Fermi surface in extremely dense plasmas, as well as to the upshifting of the K-edge.

To test if the traditional density-dependent continuum-lowering models can explain these observations, we plot the different predictions of the carbon K-edge as a function of the ion charge state Z (or plasma density) in Fig. 3. Four IPD models including Ecker–Kröll,[1] Stewart–

Pyatt,[2] modified ion sphere,[3] and Crowley[4] (represented by the various curves with open squares) were used to calculate the K-edges versus the ion charge state (Z = 1 to 5). Once again, the K-edge for an ion charge state was calculated in these models by $E_{\text{K-edge}} = E_{\text{C}} - E_{1s}$, with E_{C} being the model-predicted IPD and E_{1s} the 1s-electron ionization potential of isolated carbon ion with a charge of Z. As can be seen from Fig. 3, the first three models predict the K-edge downshifting as Z/ρ increases; while the Crowley model, considering the degeneracy-induced increase in Fermi energy, qualitatively gives some upshifting of the K-edge, but only for the case of Z = 5. Dramatically different from all these model predictions, our QMD results (blue circles) show significant upshifts for $\rho \geq 50$ g/cm^3. Note that our QMD calculations do not assume what ionization level is reached for each density studied. We therefore plotted these QMD results by using the up x axis of plasma density, while the down x axis of the ion charge state was estimated by using the average-atom model[46]. In Fig. 3, the QMD-predicted K-edges are located at 270, 272.5, 286.0, 317.8, 385.3, and 442.5 eV, respectively, for carbon plasma densities of ρ = 3.5, 10, 25, 50, 100, and 150 g/cm^3. Since it is a well-known problem for DFT using the Perdew–Burke–Ernzerhof (PBE) exchange-correlation functional[43] (currently adopted in our QMD calculations), the resulting band gap is somewhat underestimated in general. We saw a K-edge deficit of ~12 eV in our DFT calculations when comparing the case of solid high-density carbon (ρ = 3.5 g/cm^3 and T = 300 K) with experiment. For this reason, we have added the constant deficit of δE = 11.77 eV (independent of density/temperature) to our QMD results shown in Fig. 3 and have assigned an "error bar" of this amount (11.77 eV) to all of them. Back to the comparison in Fig. 3, our *ab initio* calculation gives a carbon K-edge at ~397 eV for the case of ρ = 100 g/cm^3. Respectively, the Stewart–Pyatt model predicts it to be $E_{\text{K-edge}} \approx 175$ eV; the

modified ion-sphere model gives $E_{\text{K-edge}} \approx 53$ eV; the Crowley model predicts $E_{\text{K-edge}} \approx 254$ eV; and the Ecker–Kröll model predicts an unphysical "negative" carbon K-edge at this density ($\rho = 100$ g/cm^3) and temperature ($T = 15{,}625$ K). To fully understand the physics behind the K-edge upshifting observed in our *ab initio* calculations, we have developed the SAIB model (more details below). This simple SAIB model's predictions, represented by the solid red line in Fig. 3, agree very well with our *ab initio* calculations.

The "single-atom-in-box" (SAIB) model: To understand the K-edge shifting in strongly coupled and fully degenerate plasmas, we have proposed the SAIB model, which consists of three pieces of physics: (1) The continuum-lowering effect on the 1*s*-electron binding energy E_{1s}; (2) the degree of ionization Z determined by an average-atom model;[46] and (3) the rising of the electronic Fermi surface calculated by $E_{\text{F}} = \left(\hbar^2/2m\right)\left(3\pi^2 \times Z \times \rho / A_{\text{C}}\right)^{2/3}$. To determine the 1*s*-electron binding energy E_{1s} at a carbon density ρ, we placed a single carbon atom inside a cubic box having a volume of $V = L^3 = A_{\text{C}}/\rho$. Using the periodic boundary condition, this SAIB picture mimics the microscopic environment of each individual carbon atom experienced in such dense plasmas. We then calculated E_{1s} by self-consistently solving the following Kohn–Sham equation for all N_{b} electronic orbitals (in atomic units):

$$\left[-\frac{1}{2}\nabla^2 - \frac{6}{r} + V_{\text{H}}[\rho_{\text{e}}](\boldsymbol{r}) + V_{xc}[\rho_{\text{e}}](\boldsymbol{r})\right]\psi_i(\boldsymbol{r}) = E_i\psi_i(\boldsymbol{r}) \qquad (1)$$

with the electron density and the Hartree term defined as:

$$\rho_{\mathrm{e}}(\boldsymbol{r}) = \sum_{i=1}^{N_b} |\psi_i(\boldsymbol{r})|^2; \quad V_{\mathrm{H}}[\rho_{\mathrm{e}}](\boldsymbol{r}) = \int \frac{\rho_{\mathrm{e}}(\boldsymbol{r}')}{|\boldsymbol{r}-\boldsymbol{r}|} \mathrm{d}\boldsymbol{r}'. \tag{2}$$

Since the exchange-correlation term V_{xc} and the Hartree term depend on the electron density $\rho_{\mathrm{e}}(\boldsymbol{r})$, which is again a function of $\psi_i(\boldsymbol{r})$, the Kohn–Sham equation can be solved in self-consistent (i.e., iterative) way. As is being used in our many-atom QMD calculations, we adopted the PBE exchange-correlation functional in the above E_{1s} calculations. To determine the average ionization Z, we employed the average-atom model with local-density approximation for the exchange-correlation functional. The resulting Z was then used to calculate the elevated Fermi surface. Finally, the K-edge locations were computed for each carbon density via $E_{\text{K-edge}} = E_{\mathrm{F}} - E_{1s}$ (note the continuum is also set to $E_{\mathrm{C}} = 0$ in our Kohn–Sham DFT calculations). As an example, the SAIB results are plotted in Fig. 3 by the solid red line (see Table I of **Supplemental Material**[38]).

For the same reason discussed above, the DFT-predicted binding energy of 1*s* electrons in the SAIB model is also underestimated. Therefore, we have overall upshifted the SAIB-predicted K-edges by the same amount of energy δE = 11.77 eV (as we did for the QMD results), which are plotted by the red solid line in Fig. 3. We see that this simple model is in very good agreement with our QMD results. It demonstrates that the SAIB model perfectly predicts the continuum lowering of atomic ions being affected by surrounding ions/electrons in these dense plasmas (even though plasma structures are ignored). Moreover, the rise in the Fermi surface, estimated from the average-atom model, captures the essence of electron degeneracy in such systems. While the existing models failed to predict the K-edge locations in such strongly coupled and

fully degenerate plasmas, we anticipate that the simple SAIB model could find important applications in studying HED properties of extremely dense plasmas.

To further investigate how the plasma temperature can affect K-edges, we increased the carbon plasma temperature from T = 15,625 K to T = 125,000 K for the case of ρ = 100 g/cm^3. The QMD results are presented in Fig. 4, in which the density of state and the x-ray absorption spectrum are displayed in Figs. 4a and 4b, respectively. Compared to the low-T case, the rising of plasma temperature broadens both the 1s band and the "quasi-bound" 2s band (see Fig. 4a). As a consequence, the K-edge gets smeared and becomes less sharp, as seen in Fig. 4b. Nevertheless, the K-edge peak location does not move with increased temperature. Note that for this high compression, the quasi-bound 2s band (or the so-called "resonance in continuum"), around E_{2s} = 148 eV at the low-T case "melts" as the plasma temperature increases to T = 125,000 K (see Fig. 4a). As a result, the previously seen absorption bump around $h\nu = E_F – E_{2s} \approx$ 160 eV at T = 15,625 K disappears in Fig. 4b. A similar absorption "bump" caused by the quasi-bound 2s band was also seen in Figs. 1b and 2b for the case of ρ = 50 g/cm^3.

In conclusion, the proposed SAIB model gives quantitative results about the K-edge of extremely dense plasmas, in very good agreement with *ab initio* QMD calculations. It points out that K-edges in strongly coupled and degenerate plasmas are determined by the competition between the lowering of continuum and the rising of the Fermi surface caused by high compressions. In contrast to such a simple SAIB model, the existing models failed to predict the correct K-edges of extremely dense plasmas. We anticipate that the physics revealed here could stimulate immediate precision-experiments to benchmark the predicted unusual K-edge shifting in strongly coupled and degenerate plasmas, widely existing in ICF targets, in stars, and the interior of planets.

Acknowledgment

This material is based upon work supported by the Department of Energy National Nuclear Security Administration under Award Number DE-NA0001944, the University of Rochester, and the New York State Energy Research and Development Authority.

References

1. Ecker, G. & Kröll, W. Lowering of the ionization energy for a plasma in thermodynamic equilibrium. *Phys. Fluids* **6**, 62–69 (1963).
2. Stewart, J. C. & Pyatt, K. D., Jr. Lowering of ionization potentials in plasmas. *Astrophys. J.* **144**, 1203–1211 (1966).
3. Liberman, D. & Albritton, J. Dense plasma equation of state model. *J. Quant. Spectrosc. Radiat. Transf.* **51**, 197–200 (1994).
4. Crowley, B. J. B. Average-atom quantum-statistical cell model for hot plasma in local thermodynamic equilibrium over a wide range of densities. *Phys. Rev. A* **41**, 2179–2191 (1990).
5. Iglesias, C. A. & Rogers, F. J. Opacities for the solar radiative interior. *Astrophys. J.* **371**, 408–417 (1991).
6. Rose, S. J. Calculations of the radiative opacity of laser-produced plasmas. *J. Phys. B: At. Mol. Opt. Phys.* **25**, 1667–1681 (1992).
7. Bailey, J. E. *et al.* A higher-than-predicted measurement of iron opacity at solar interior temperatures. *Nature* **517**, 56–59 (2015).
8. Hansen, S. B. *et al.* Temperature determination using Kα spectra from *M*-shell Ti ions. *Phys. Rev. E* **72**, 036408 (2005).
9. Vinko, S. M. *et al.* Creation and diagnosis of a solid-density plasma with an x-ray free-electron laser. *Nature* **482**, 59–62 (2012).
10. Ciricosta, O. *et al.* Direct measurements of the ionization potential depression in a dense plasma. *Phys. Rev. Lett.* **109**, 065002 (2012).

11. Vinko, S. M., Ciricosta, O. & Wark, J. S. Density functional theory calculations of continuum lowering in strongly coupled plasmas. *Nat. Commun.* **5**, 3533 (2014).

12. Hoarty, D. J. *et al.* Observations of the effect of ionization-potential depression in hot dense plasma. *Phys. Rev. Lett.* **110**, 265003 (2013).

13. Fletcher, L. B. *et al.* Observations of continuum depression in warm dense matter with x-ray Thomson scattering. *Phys. Rev. Lett.* **112**, 145004 (2014).

14. Ciricosta, O. *et al.* Measurements of continuum lowering in solid-density plasmas created from elements and compounds. *Nat. Commun.* **7**, 11713 (2016).

15. Hansen, S. B. *et al.* Detailed analysis of hollow ions spectra from dense matter pumped by x-ray emission of relativistic laser plasma. *Phys. Plasmas* **21**, 031213 (2014).

16. Crowley, B. J. B. Continuum lowering – A new perspective. *High Energy Density Phys.* **13**, 84–102 (2014).

17. Son, S.-K., Thiele, R., Jurek, Z., Ziaja, B. & Santra, R. Quantum-mechanical calculation of ionization-potential lowering in dense plasmas. *Phys. Rev. X* **4**, 031004 (2014).

18. Iglesias, C. A. A plea for a reexamination of ionization potential depression measurements. *High Energy Density Phys.* **12**, 5–11 (2014).

19. Mazevet, S. & Zérah, G. *Ab initio* simulations of the *K*-edge shift along the aluminum hugoniot. *Phys. Rev. Lett.* **101**, 155001 (2008).

20. Cho, B. I. *et al.* Electronic structure of warm dense copper studied by ultrafast x-ray absorption spectroscopy. *Phys. Rev. Lett.* **106**, 167601 (2011).

21. Zhang, S., Zhao, S., Kang, W. N., Zhang, P. & He, X.-T. Link between *K* absorption edges and thermodynamic properties of warm dense plasmas established by an improved first-principles method. *Phys. Rev. B* **93**, 115114 (2016).

22. Booth, N. *et al.* Laboratory measurements of resistivity in warm dense plasmas relevant to the microphysics of brown dwarfs. *Nat. Commun.* **6**, 8742 (2015).

23. Rose, S. J. New experimental possibilities for measuring radiative opacity under conditions in the sun's interior. *Plasma Phys. Control. Fusion* **47**, B735–B741 (2005).

24. Seager, S. Exoplanet habitability. *Science* **340**, 577–581 (2013).

25. Hu, S. X., Militzer, B., Goncharov, V. N. & Skupsky, S. Strong coupling and degeneracy effects in inertial confinement fusion implosions. *Phys. Rev. Lett.* **104**, 235003 (2010).

26. Caillabet, L., Canaud, B., Salin, G., Mazevet, S. & Loubeyre, P. Change in inertial confinement fusion implosions upon using an *ab initio* multiphase DT equation of state. *Phys. Rev. Lett.* **107**, 115004 (2011).

27. Hu, S. X. *et al.* Impact of first-principles properties of deuterium-tritium on inertial confinement fusion target designs. *Phys. Plasmas* **22**, 056304 (2015).

28. Glenzer, S. H. & Redmer, R. X-ray thomson scattering in high energy density plasmas. *Rev. Mod. Phys.* **81**, 1625–1663 (2009); Drake, R. P. Perspectives on high-energy-density physics. *Phys. Plasmas* **16**, 055501 (2009).

29. Kohn, W. & Sham, L. J. Self-consistent equations including exchange and correlation effects. *Phys. Rev.* **140**, A1133–A1138 (1965).

30. Mermin, N. D. Thermal properties of the inhomogeneous electron gas. *Phys. Rev.* **137**, A1441–A1443 (1965).

31. Collins, L., Kwon, I., Kress, J., Troullier, N. & Lynch, D. Quantum molecular dynamics simulations of hot, dense hydrogen. *Phys. Rev. E* **52**, 6202–6219 (1995).

32. Clérouin, J. G. & Bernard, S. Dense hydrogen plasma: Comparison between models. *Phys. Rev. E* **56**, 3534–3539 (1997).

33. Collins, L. A. *et al.* Dynamical and optical properties of warm dense hydrogen. *Phys. Rev. B* **63**, 184110 (2001).

34. Clérouin, J. & Dufrêche, J.-F. *Ab initio* study of deuterium in the dissociating regime: Sound speed and transport properties. *Phys. Rev. E* **64**, 066406 (2001).

35. Desjarlais, M. P. Density-functional calculations of the liquid deuterium Hugoniot, reshock, and reverberation timing. *Phys. Rev. B* **68**, 064204 (2003).

36. Holst, B., Redmer, R. & Desjarlais, M. P. Thermophysical properties of warm dense hydrogen using quantum molecular dynamics simulations. *Phys. Rev. B* **77**, 184201 (2008).

37. Recoules, V., Lambert, F., Decoster, A., Canaud, B. & Clérouin, J. *Ab initio* determination of thermal conductivity of dense hydrogen plasmas. *Phys. Rev. Lett.* **102**, 075002 (2009).

38. See Supplemental Material at http://xxx for a more detailed description of the computational method and convergence tests, which includes Refs. [39-45].

39. Kresse, G. & Hafner, J. *Ab initio* molecular dynamics for liquid metals. *Phys. Rev. B* **47**, 558–561 (1993).

40. Kresse, G. & Hafner, J. *Ab initio* molecular-dynamics simulation of the liquid-metal–amorphous-semiconductor transition in germanium. *Phys. Rev. B* **49**, 14251–14269 (1994).

41. Kresse, G. & Furthmüller, J. Efficient iterative schemes for *ab initio* total-energy calculations using a plane-wave basis set. *Phys. Rev. B* **54**, 11,169–11,186 (1996).

42. Kubo, R. Statistical-mechanical theory of irreversible processes. I. General theory and simple applications to magnetic and conduction problems. *J. Phys. Soc. Jpn.* **12**, 570–586

(1957); Greenwood, D. A. The Boltzmann equation in the theory of electrical conduction in metals. *Proc. Phys. Soc. Lond.* **71**, 585–596 (1958).

43. Perdew, J. P., Burke, K. & Ernzerhof, M. Generalized gradient approximation made simple. *Phys. Rev. Lett.* **77**, 3865–3868 (1996).

44. Perrot, F. New approximation for calculating free-free absorption in hot dense plasmas. *Laser Part. Beams* **14**, 731–748 (1996).

45. Hu, S. X. *et al.* First-principles opacity table of warm dense deuterium for inertial-confinement-fusion applications. *Phys. Rev. E* **90**, 033111 (2014).

46. Liberman, D. A. Self-consistent field model for condensed matter. *Phys. Rev. B* **20**, 4981–4989 (1979); Lambert, F., Clérouin, J. & Zérah, G. Very-high-temperature molecular dynamics. *Phys. Rev. E* **73**, 016403 (2006).

Figure captions

Figure 1. (Color online) The mass absorption coefficient α_m as a function of photon energy ($h\nu$) for extremely compressed carbon at a temperature of T = 15,625 K but different densities of (a) ρ = 10 g/cm^3, (b) ρ = 50 g/cm^3, (c) ρ = 100 g/cm^3, and (d) ρ = 150 g/cm^3. The black arrow in each panel marks the location of the carbon K-edge in such extremely dense plasmas.

Figure 2. (Color online) The electronic density of state (DOS) as a function of the band energy, for the four cases corresponding to Fig. 1. The dashed black line in each panel marks the location of the Fermi energy.

Figure 3. (Color online) The QMD-predicted K-edges of carbon plasmas as a function of the corresponding ion charge state Z (or the mass density), in comparison with predictions from various continuum-lowering models of Ecker–Kröll,[1] Stewart–Pyatt,[2] modified ion sphere,[3] and Crowley.[4] The proposed simple model SAIB ("single atom in box") accurately predicts the correct K-edge positions.

Figure 4. (Color online) (a) The electronic density of state (DOS) as a function of the band energy, for the dense carbon plasma of ρ = 100 g/cm^3 at two different temperatures of T = 15,625 K (blue solid) and T = 125000 K (red dashed). (b) The corresponding photoabsorption spectra. The temperature induced broadening of the 1s-band in (a) is indicated by the less-sharp K-edge in the absorption spectrum.

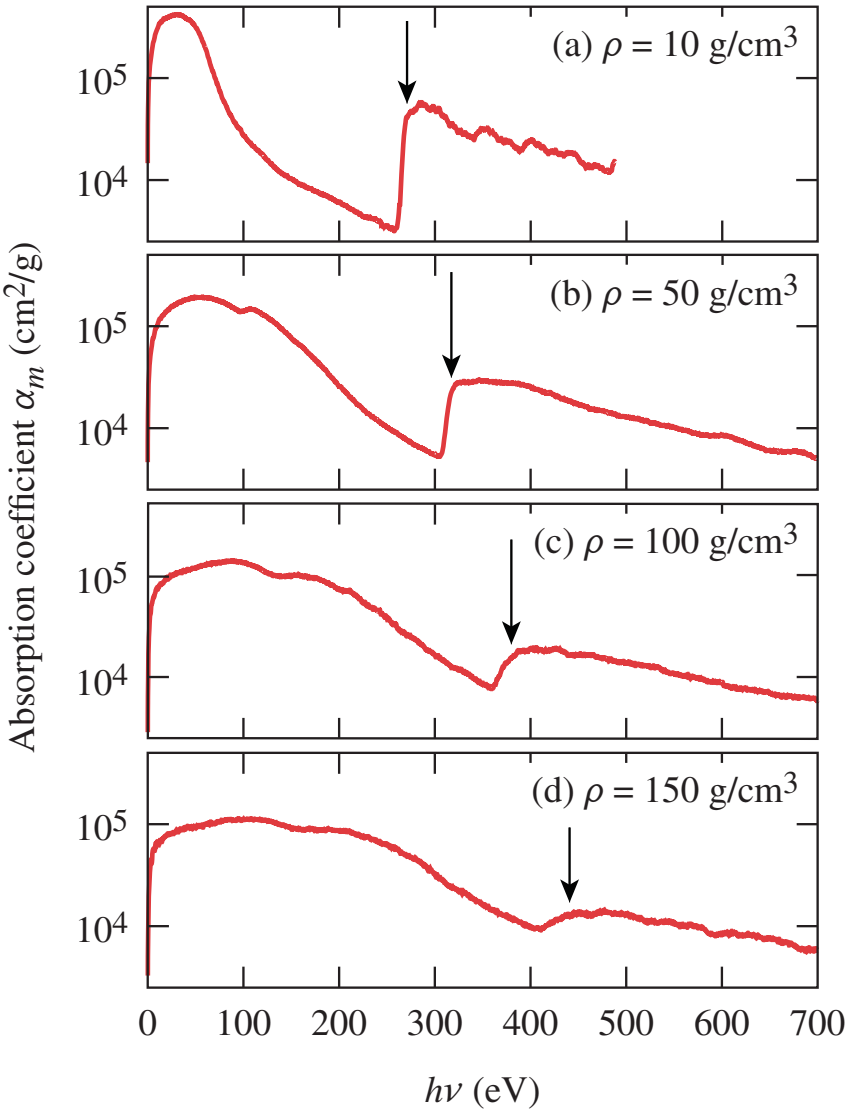

Figure 1. (Color online) The mass absorption coefficient α_m as a function of photon energy ($h\nu$) for extremely compressed carbon at a temperature of T = 15,625 K but different densities of (a) ρ = 10 g/cm^3, (b) ρ = 50 g/cm^3, (c) ρ = 100 g/cm^3, and (d) ρ = 150 g/cm^3. The black arrow in each panel marks the location of the carbon K-edge in such extremely dense plasmas.

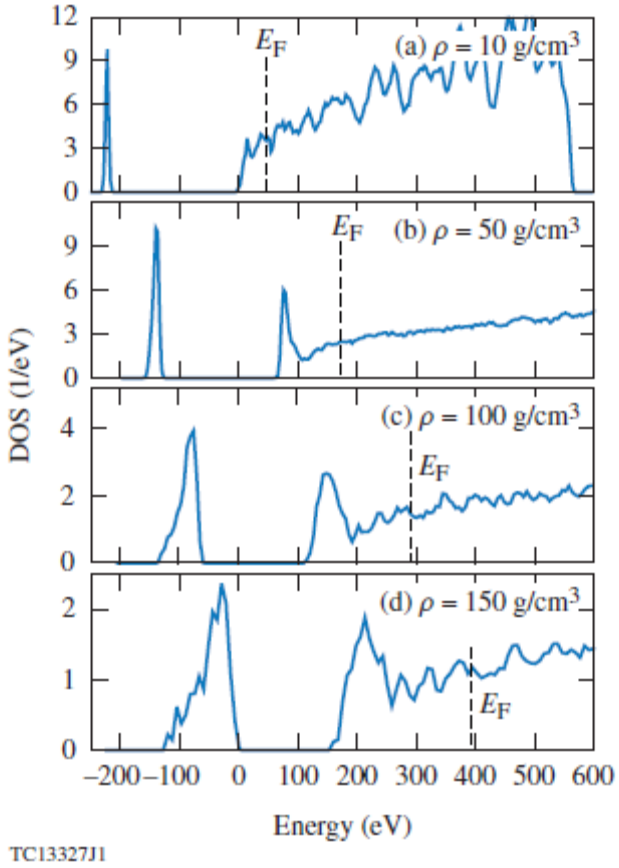

Figure 2. (Color online) The electronic density of state (DOS) as a function of the band energy, for the four cases corresponding to Fig. 1. The dashed black line in each panel marks the location of the Fermi energy.

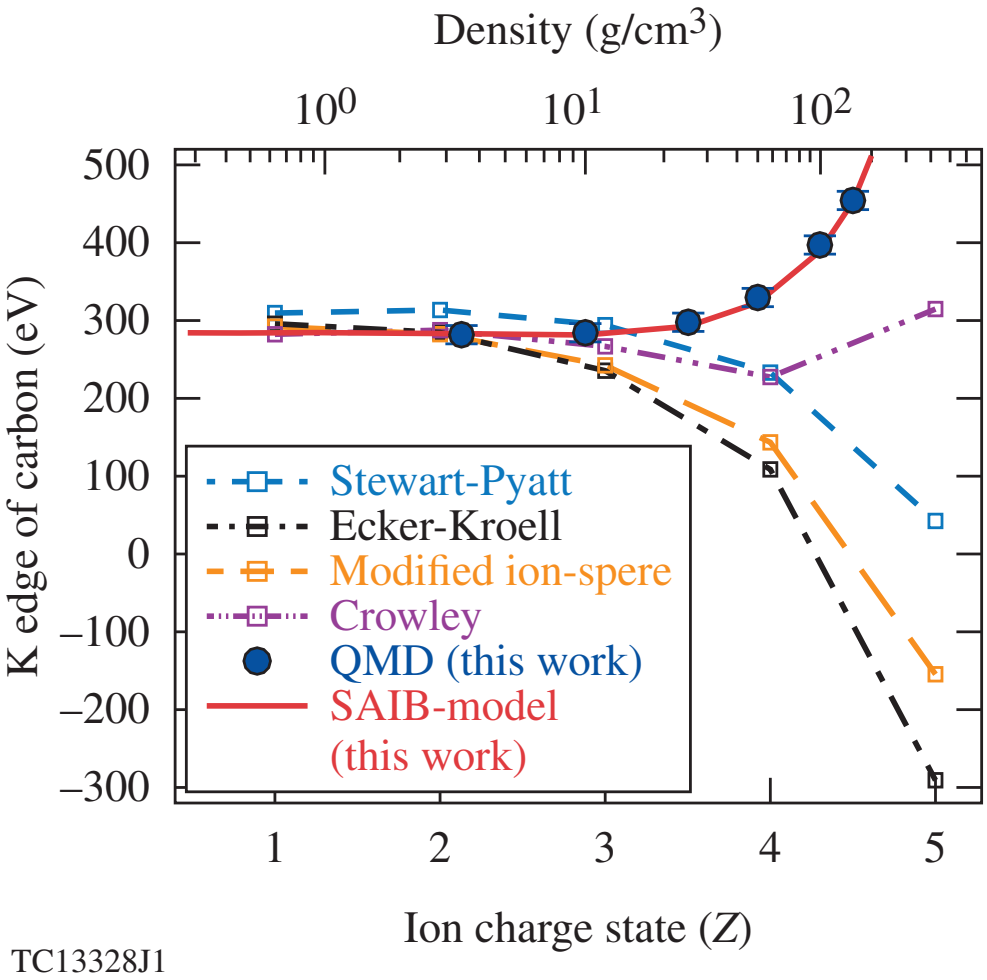

Figure 3. (Color online) The QMD-predicted K-edges of carbon plasmas as a function of the corresponding ion charge state Z (or the mass density), in comparison with predictions from various continuum-lowering models of Ecker–Kröll,[1] Stewart–Pyatt,[2] modified ion sphere,[3] and Crowley.[4] The proposed simple model SAIB ("single atom in box") accurately predicts the correct K-edge positions.

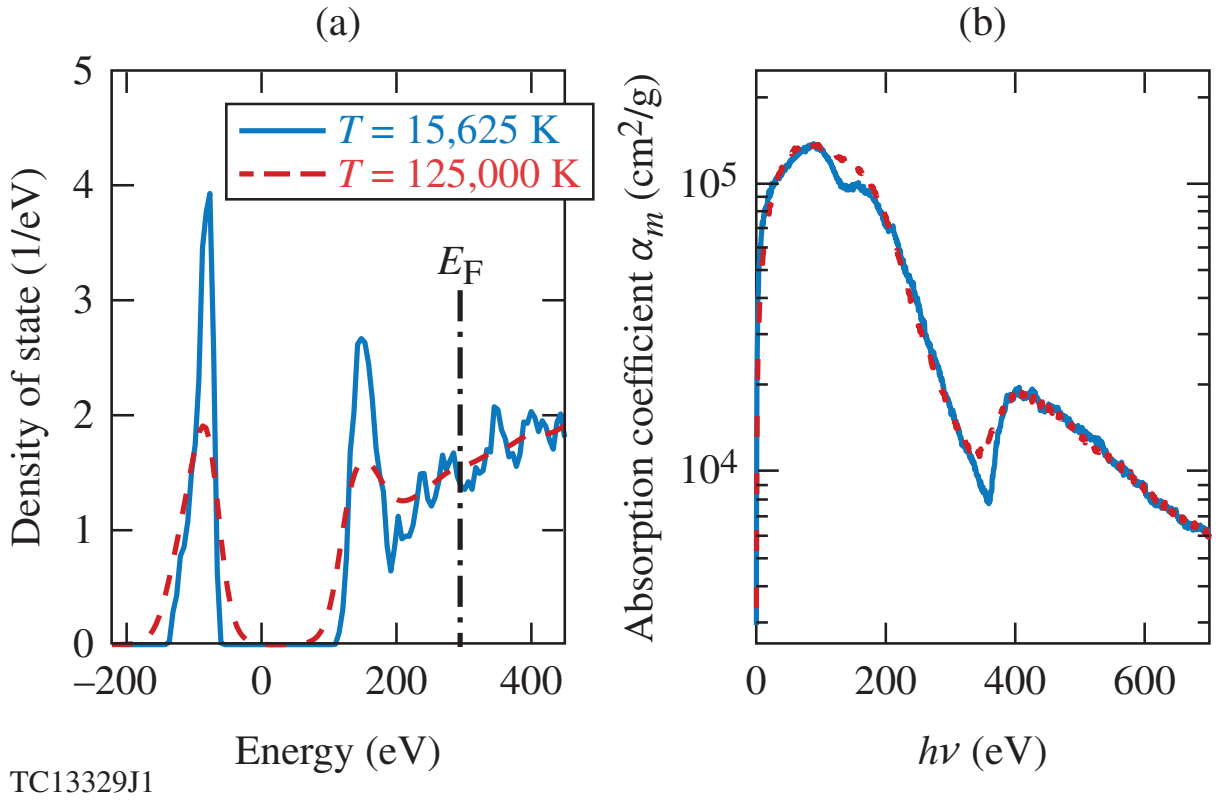

Figure 4. (Color online) (a) The electronic density of state (DOS) as a function of the band energy, for the dense carbon plasma of ρ = 100 g/cm^3 at two different temperatures of T = 15,625 K (blue solid) and T = 125000 K (red dashed). (b) The corresponding photoabsorption spectra. The temperature induced broadening of the 1*s*-band in (a) is indicated by the less-sharp K-edge in the absorption spectrum.